FOCUSED ISSUE FEATURE

Nanoelectronics-Based Integrated Antennas

Peter Russer, Nikolaus Fichtner, Paolo Lugli, Wolfgang Porod, Johannes A. Russer, and Hristomir Yordanov

Peter Russer (russer@tum.de), Nikolaus Fichtner, Paolo Lugli, Johannes A. Russer, and Hristomir Yordanov are with Institute for Nanoelectronics, Technische Universität München, Arcisstrasse 21, 80333 Munich, Germany. Wolfgang Porod (porod@nd.edu) is with the Center for Nano Science and Technology, University of Notre Dame, Indiana 46556 USA.

Digital Object Identifier 10.1109/MMM.2010.938570

 1527-3342/10/$26.00©2010 IEEE

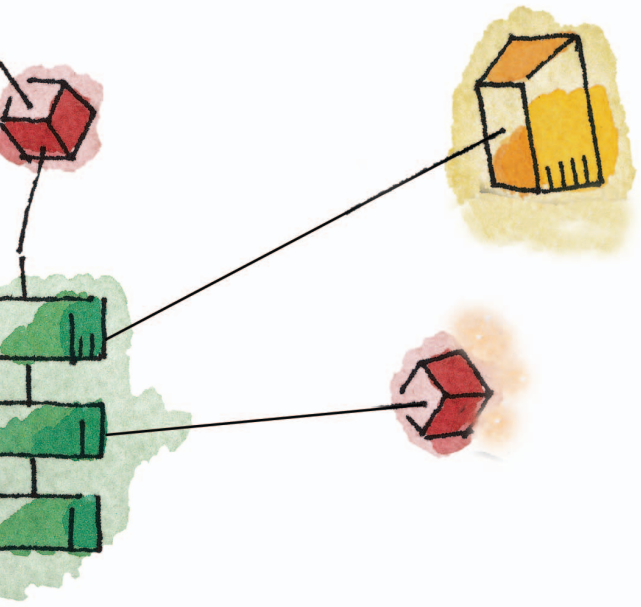

Integrated nanolectronics-based antennas provide interesting possibilities for short-range data transfer such as wireless chip-to-chip or intrachip communication.

Nanoelectronics is the gateway to a variety of novel electronic devices and systems with substantially new properties. It enables the development of nanoscale electronic devices, covering radio frequencies in the terahertz range and beyond up to optical frequencies [1]–[3]. The on-chip integration of antennas opens new vistas for novel devices and integrated systems for sensing, detection, wireless communications, and energy harvesting applications. However, the requirements of antenna integration into the chip architecture are different from those of circuit integration. Nanoelectronic technologies strike a compromise between these requirements.

Today, silicon and silicon-germanium-based monolithic integrated millimeter-wave (mm-wave) circuits already facilitate the realization of communication and sensing systems operating at frequencies up to the mm-wave range [4], [5]. In the near future, Si-based integrated circuits (ICs) will open up new perspectives in communication and sensor technologies. In this context, monolithic integration of antennas contributes significantly to the compactness of front ends and avoids lossy and expensive cable connections between circuitry and antennas [6]. At mm-wave frequencies and beyond, the antenna dimensions are small enough so that even antenna arrays may be integrated monolithically.

Besides developments in semiconductor technology, the emerging possibility for integration of antennas within future nanoelectronic device platforms based, for example, on polymer materials, carbon nanotubes (CNTs), graphene, superconductors, or plasmonic devices, opens up interesting perspectives. The electronic properties of some materials will allow an extreme miniaturization of antennas. For physical reasons, frequencies ranging from the terahertz region up into the optical region require close integration of the active or rectifying device. Furthermore, in some cases, the electronic properties of the antenna material and structures are essential for the operation of the antenna. Examples for this are CNT antennas, nanowire antennas, plasmonic antennas, and some metallic and superconducting antenna structures. We distinguish between nanoelectronics-based integrated antennas and nanoantennas. The former are motivated by the requirements of a nanoelectronic monolithic IC or system-on-chip. Nanoantennas are nanostructures themselves. The design of nanoelectronic systems-on-chip with integrated antennas or nanoantennas should be performed by combining methods of antenna design and nanoelectronic device design.

In this overview, we first discuss the physical constraints limiting the realization of small antennas and their integration into monolithic circuits. Then we discuss the conditions and possibilities for monolithic integration of antennas into semiconductor-based monolithic ICs. Next, we consider the possible realization of monolithic ICs in connection with novel materials and devices. In the "Integration of Antennas with Metal-Oxide-Metal Diodes" section, we discuss antenna structures with metal-oxide-metal (MOM) diodes, and then we discuss antennas in plasmonic devices. The next section deals with superconducting antennas which, based on various principles, facilitate design solutions for applications from low frequencies up to the optical frequency range. The sections after that deal with CNT antennas and graphene antennas. Finally, alternative materials and fabrication techniques are discussed.

Physical Constraints in Antenna Integration

The monolithic integration of antennas imposes severe restrictions on the chip area used by the antenna. In order to clarify the requirements for the monolithic integration of the antenna, it is necessary to consider the fundamental physical limitations of antennas. In

Note: This article will also appear in the December 2010 issue of *IEEE Antennas and Propagation Magazine*.

1948, L.J. Chu discussed the physical limitations of omnidirectional antennas showing that an antenna embedded in a virtual sphere with diameter $2a$, and hence, exhibiting a maximum dimension of $2a$, has a potentiality of a broad bandwidth under the condition that the antenna gain is equal or less than $4a/\lambda$ [7].

H.A. Wheeler introduced the concept of the *radiation power factor* to evaluate the radiation of real power from a small antenna [8]–[11] and discussed the effective volumes of various antenna shapes [9]. Physical limitations of bandwidth, gain, and directivity have been derived for antennas of arbitrary shape [12], [13]. We would like to stress that, as Schelkunoff has shown in 1943, arbitrarily high gain can be obtained from an antenna array of given overall length [14]. Superdirectivity antennas, however, require extremely high currents to produce only a small radiation field [15].

Integrated nanolectronics-based antennas provide interesting possibilities for short-range data transfer such as wireless chip-to-chip or intrachip communication. Wireless on-chip communication and chip-to-chip communication may be a solution to the increasing complexity and density of interconnect structures of monolithic ICs. Ultrawideband (UWB) technology offers high data rates over short distances without suffering from the multipath interferences and, therefore, will be suitable for this purpose. Chips may include planar antenna structures, forming a multiple-input and multiple-output (MIMO) system. MIMO transmission provides a significant increase in data throughput and link range without additional bandwidth or transmit power due to its higher spectral efficiency and link diversity [16], [17]. Figure 1 shows a wireless MIMO channel model where each receiving antenna $RX_1 \ldots RX_3$ receives the signal of every transmitting antenna $TX_1 \ldots TX_3$. Figure 2 shows two chips, each with several antenna elements. The mutual electromagnetic coupling of the antenna elements occurs both between the antenna elements of a chip and between the antenna elements of different chips. The electromagnetic coupling can be performed via waves radiated into space and surface waves along the chip surface. The coupling also is affected by the housing assembly and by scattering bodies.

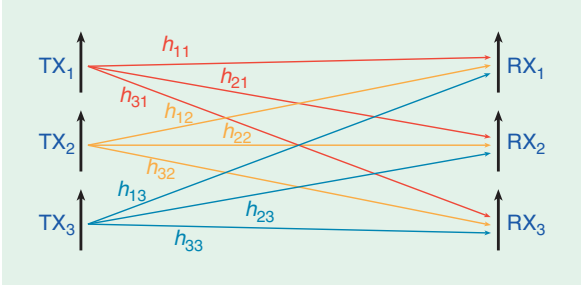

Figure 1. *The wireless MIMO channel model.*

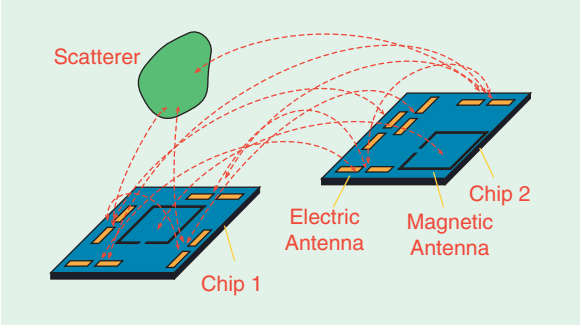

Figure 2. *Interchip and intrachip MIMO communication.*

If the antennas at one side of the transmission link are confined within a limited space, the maximum number N of useful channels according to [17] is limited by

$$N = 8\pi^2 \frac{a^2}{\lambda^2}, \tag{1}$$

where a is the radius of the smallest sphere enclosing the antennas at the ends of the link. A rigorous network theoretic framework for MIMO channels is given in [18].

The Shannon information capacity of space-time wireless channels formed by electromagnetic sources and receivers in a known background medium is analyzed in [19] from the fundamental physical point of view of Maxwell's equations. For a given additive Gaussian noise model, the information capacity is bounded, depending on the spherical volume enclosing the receiver antennas. A circuit theoretic multiport model for the design of the wireless MIMO communication link for optimum capacity is presented in [20]. In this article we show that the channel matrix used in the information theoretic context can be derived from multiport circuit models. This channel matrix can have full rank and therefore support multistream transmission, even if the antennas are densely packed. This work is of fundamental importance for the realization of chip to chip transmission links.

Monolithic Integrated Antennas

Today, silicon is the most interesting basic material for the monolithic integration of antennas. The monolithic integration of antennas has to be realized in such a way that the electromagnetic wave is emitted with high efficiency, is attenuated through the substrate as little as possible, and does not excite substrate waves. Since monolithic integrated antennas on the chip area are in close proximity to the circuitry, and even sometimes share an area with it, the design of the IC has to be such that the antenna radiation field does not interfere with the guided waves in the circuits and interconnects.

Silicon as a substrate for mm-wave monolithically ICs has been suggested in 1981, when no one believed in the applicability of silicon in this frequency range, by the RCA group of A. Rosen [21]. There have been

research activities since 1985 in the field of silicon mm-wave ICs (SIMMWICs) at the former AEG-Telefunken Research Institute (which became the Daimler Research Center) and at the Technische Universität München [22]. It has been shown that high-resistivity silicon with a resistivity greater than 2,000 $\Omega \cdot$ cm is excellently suited for monolithic integration of RF circuits at frequencies above 40 GHz since substrate losses can be neglected in comparison with skin effect losses and radiation losses. Planar transmitters and receivers for frequencies up to 100 GHz with integrated antenna structures have been realized [6], [22], [23]. The requirement to use high-resistivity silicon as the substrate for fabricating distributed passive circuit structures and antennas determines the design philosophy of SIMMWICs.

Today, a vast literature exists on monolithic integrated antennas. Using a 0.18 μm CMOS copper technology, a 15 GHz on-chip wireless interconnect system, integrating antennas in digital CMOS circuitry facilitating wireless clock distribution over the chip, has been presented in [24], [25]. A 15 GHz intrachip wireless interconnect using integrated antennas consisting of a transmitter-receiver pair fabricated in 0.18 μm CMOS technology is described in [26]. Further work on wireless interchip communication has been presented in [27], [28], where a transmitter and receiver pair were fabricated in a 0.18 μm CMOS process. In this work, a 15 GHz sine wave was transmitted from an on-chip 2 mm long zigzag dipole antenna and received by a zigzag dipole antenna located 2.2 cm away. An intrachip wireless interconnect system using meander monopole on-chip antennas and operating in a frequency band from 22 GHz–29 GHz is described in [29]. On-chip UWB radios in that frequency band are discussed there. The on-chip antennas are meander monopoles with 1 mm axial length, as depicted in Figure 3.

Monopole antennas have been fabricated on high- and low-resistivity substrates and measured up to 110 GHz [30]. Measurements of monopoles at frequencies up to 110 GHz have shown that antennas on high-resistivity substrates have a much higher transmission coefficient than those on low-resistivity material. Channel modeling of wireless interchip and intrachip communication has been performed in [31].

One problem in monolithic integration of antennas is the high chip-area demand of antenna structures, which would drive up the costs of chips with integrated antennas. In [32] and [33], the utilization of the electronic circuit ground planes as radiating elements for the integrated antennas has been proposed. This allows for optimal usage of chip area, as the antennas share the chip area with the circuits. Care should be taken that the interference between the antenna field and the field propagating in the circuit structures stays within tolerable limits. The structure represented schematically in

Today, silicon is the most interesting basic material for the monolithic integration of antennas.

Figure 4 contains two antenna patches. Both antenna patches serve as the ground planes of the circuits. These circuits contain line drivers $T_1 \ldots T_4$ driving over symmetrical interconnection lines the line receivers $R_1 \ldots R_4$. Furthermore, there is a driver T_A, the output of which is connected to both patches: however, only one conductor bridges the gap between the patches. The sum of the currents $i_1 \ldots i_4$ flowing in both directions through the transmission line modes vanishes and is not exciting the antenna. On the other hand, the current i_A excites an antenna radiation mode. The circuit for this current is closed via the displacement current in the near-field of the antenna. By exciting the interconnection structures in transmission line modes and the antennas in antenna modes, the interference between circuit and antennas can be minimized. We don't need to use differential lines between the patches. Any arrangement of N conductors guiding $N-1$ transmission line modes can be used. In general, an interconnection structure consisting of N conductors can guide up to $N-1$ quasi-transverse electromagnetic transmission line modes and one antenna mode.

Figure 5 shows schematically the realization of this principle in silicon technology [32], [33]. The IC is fabricated on a high-resistivity silicon substrate ($\geq$1k $\Omega \cdot$ cm) of 650 μm thickness. The substrate is backed by a metallic layer. On top of the substrate, a low-impedance layer ($\approx 5\Omega \cdot$ cm) of 5 μm thickness is grown. The

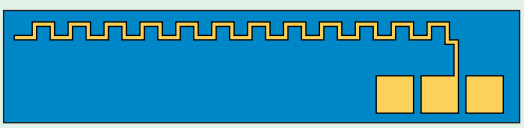

Figure 3. *On-chip meander antenna [29].*

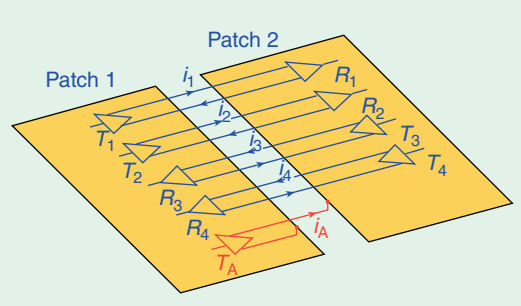

Figure 4. *Differential lines, connecting the digital circuits under the separate antenna patches.*

CMOS circuitry and the interconnects are embedded in this top layer. The low-resistivity top layer is required to achieve circuit insulation. The electromagnetic field of the circuits is mainly confined in this top layer. The antenna field is spreading over the whole thickness of the substrate. Due to the high resistivity of the substrate, the antenna losses are low. Since only a small fraction of the antenna near-field energy is stored in the low-resistivity layer, the coupling between the antenna near-field and the circuit field is weak. Furthermore, the interference between the CMOS circuits and the antenna field can be reduced when the main part of the circuit is operating in a frequency band distinct from the frequency band used for the wireless transmission.

Figure 6 shows the simulated current distribution of a two-patch V-band antenna [32], [33]. The current distribution in both patches mainly is concentrated in the neighborhood of the slots. The antenna behaves as an open-circuited slot antenna. The guided wavelength is in the range of 1 mm. The open-circuited slot with a length of about 1 mm is a transmission line resonator with a resonance frequency in the V-band. The standing wave in the slot excites the radiation field.

Figure 7 shows a photograph of the fabricated open-circuit slot antenna with CMOS circuits under the antenna electrode [33]. The measured return loss of the diced slot antenna from Figure 7 is compared with the simulation results in Figure 8.

Figure 9 shows the measured insertion loss of a wireless interchip link formed by two antennas according to Figures 6 and 7. The measurements have been performed for two antenna alignments where the antennas were positioned in each other's radiation minima and maxima. Both cases were investigated on-wafer and for diced chips. The chip-to-chip links show greater insertion loss due to the reflection on the substrate-free space interface. The worst-case transmission link gain-chip-to-chip link in the direction of

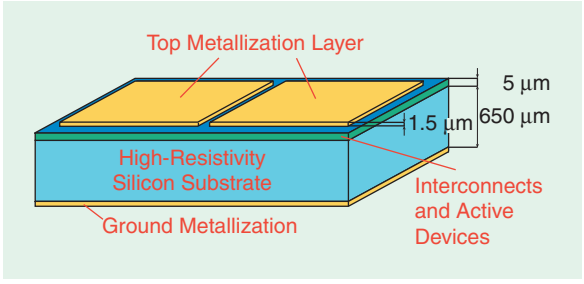

Figure 5. *Schematic drawing of a chip with an integrated antenna.*

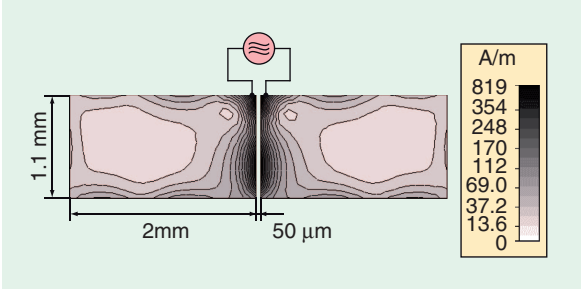

Figure 6. *Top view and current distribution of a two-patch antenna operating at 66 GHz. Reprinted with permission from [33]. (Copyright 2010, European Microwave Association.)*

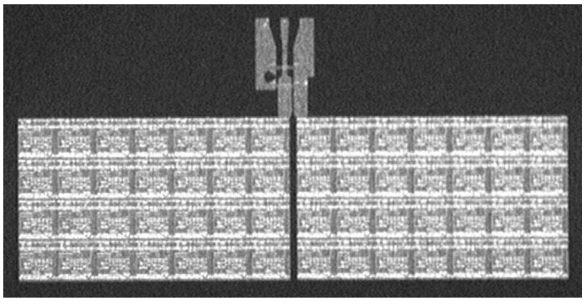

Figure 7. *Photograph of the open slot antenna. Reprinted with permission from [33]. (Copyright 2010, European Microwave Association.)*

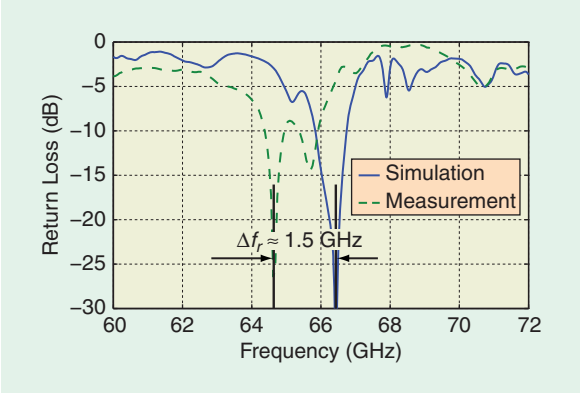

Figure 8. *Measured return loss of the on-chip open slot antenna. Reprinted with permission from [33]. (Copyright 2010, European Microwave Association.)*

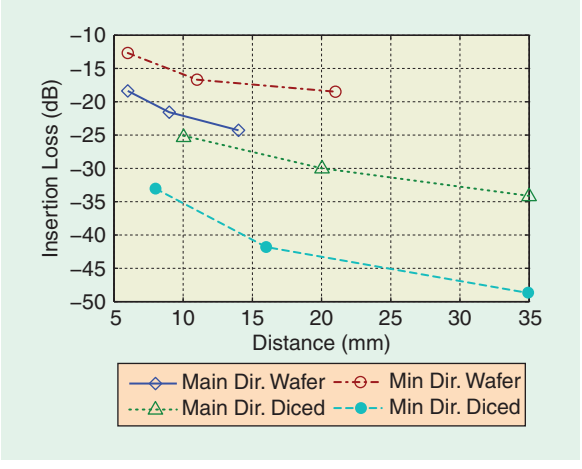

Figure 9. *Measured insertion loss of a wireless chip-to-chip link. Reprinted with permission from [33]. (Copyright 2010, European Microwave Association.)*

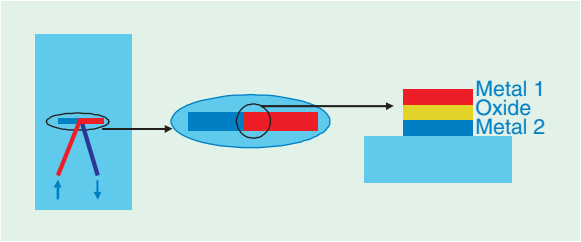

Figure 10. *Schematic diagram of a dipole antenna with integrated metal-oxide-metal diode.*

minimum radiation shows an insertion loss of –47 dB, which is sufficient for high-rate data links.

Integration of Antennas with Metal-Oxide-Metal Diodes

A promising novel concept for infrared (IR) detectors is the combination of a nanoantenna with a rectifying element. The rectifying element extracts a dc component from the rapidly varying current delivered from the nanoantenna. Semiconductor diodes are widely used, but they encounter frequency limitations for the mm-wave and long-wave IR regime. It has been demonstrated that MOM tunnel diodes can provide rectification for IR and even optical radiation [34]. A schematic diagram of a dipole antenna with an integrated MOM diode is depicted in Figure 10. Such MOM diodes are formed naturally at the overlap area between two antenna arms, for example, for a dipole antenna [35]. The early work focused on symmetrical MOM diodes, that is, diodes with the same metal for both electrodes (antenna arms). Such symmetrical MOM structures result in symmetrical current-voltage characteristics, and they need to be biased away from the origin of the I–V curve in order to yield a nonlinearity needed for rectification. This results in extra detector noise due to the bias and added circuit complexity. Recent work has shown that asymmetrical MOM diodes can be formed by metal combinations with different work functions, such as platinum and aluminum, and the resulting asymmetrical I–V curves posses the required nonlinearity for zero bias [36]. An important issue for rectification at IR frequencies is the time constant of the rectifying element. For detection of 10 μm long-wave IR radiation, the rectifying element has to be able to respond to 30 THz antenna currents. For a typical antenna resistance of 100 Ω, this limits the tunnel-diode capacitor area to less than 100 nm $\times$ 100 nm, which is challenging for fabrication. Recent work has demonstrated e-beam lithographically defined dipole antenna structures with integrated MOM diodes that showed the expected polarization response (Figure 11) and antenna-length dependence of dipole nanoantennas for 10 μm long-wave IR radiation [37], [38]. In the future, we plan to use nanoimprinting and nanotransfer techniques for the realization of the complete nanoantenna [39], [40], as discussed in the following sections.

Plasmonics deals with unique properties of metals at optical frequencies to guide and manipulate light signals at the nanoscale [41], [42].

Antennas in Plasmonic Devices

Plasmonics deals with unique properties of metals at optical frequencies to guide and manipulate light signals at the nanoscale [41], [42]. At optical frequencies, a local electric field oriented parallel to a CNT or a thin metallic wire with a diameter in the order of some nanometers can affect a local charge separation and generate quasiparticles resulting from the quantization of plasma oscillations [43].

Figure 12 shows the schematic of a nanoscale plasmonic optical antenna consisting of a metallic rod with a small gap in the center filled with a different material [44]. The antenna concentrates the received optical energy in this feedgap and yields a strong interaction with the material in the gap. The time-varying electric field due to the incident light wave can exert a force on the electrons inside the metal and drive them into a collective oscillation, known as a surface plasmon. Depending on the application, the gap can be filled by semiconducting or nonlinear metal, but also by single molecules, DNA, or protein. Even moderate illumination yields high plasmonic field intensities. Therefore, nonlinear devices for frequency conversion and

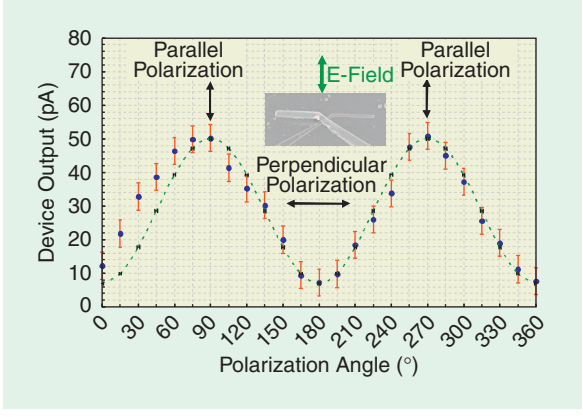

Figure 11. *Polarization-dependent response. Reprinted with permission from [37]. (Copyright 2009, American Vacuum Society.)*

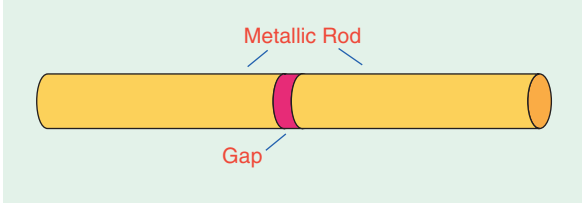

Figure 12. *Plasmonic optical antenna.*

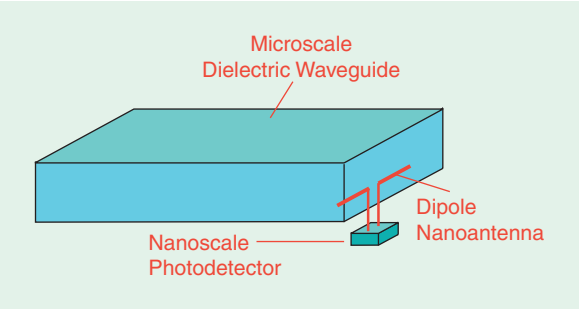

Figure 13. *Nanoantenna for coupling between microscale dielectric photonic devices and nanoscale electronics.*

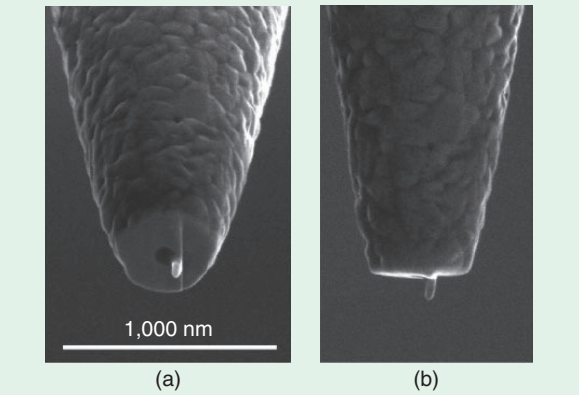

Figure 14. *Scanning electron microscope images of a probe-based nanoantenna (a) viewed from 52° angle and (b) side view [46].*

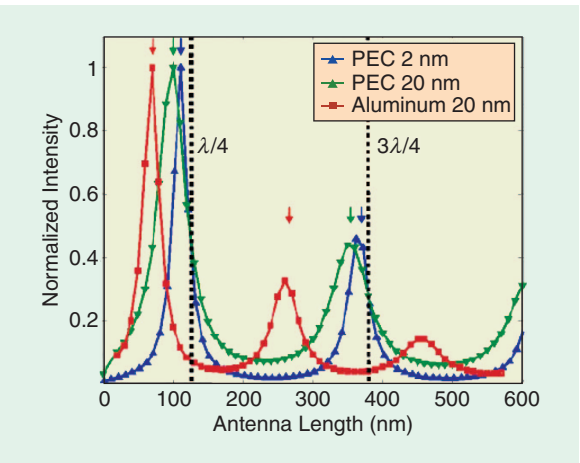

Figure 15. *Calculated field resonances [46].*

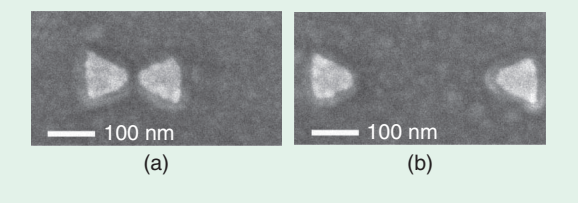

Figure 16. *Scanning electron microscope images of the bowtie antennas with gaps of (a) 20 nm and (b) 285 nm [48].*

high-speed optical switching may be realized. With semiconductors in the gap, ultrafast, low-noise photodetectors could be realized.

In [45], a silicon nanophotodiode with a surface plasmon antenna for a large-scale intigrated chip is described. A surface plasmon resonance structure is used to achieve an efficient light coupling and short response time. A silicon oxynitride (SiON) waveguide integrated structure is applied to feed the light into periodic nanoscale metal-semiconductor-metal Schottky electrodes, operating as a plasmonic optical antenna.

In [42], chip-scale optical interconnects are proposed where optical antennas are used to bridge the gap between microscale dielectric photonic devices and nanoscale electronics (Figure 13).

A resonant optical monopole nanoantenna positioned at the end of a metal-coated glass fiber near-field probe is described in [46]. Figure 14 shows the scanning electron microscope images of this antenna. The base of the nanoantenna is a fiber-optic probe whose sharp glass tip has been made by heat-pulling of the fiber. The fiber has been coated by evaporation with a few nanometer thick chromium adhesion layers, and, upon this, comes a 150 nm aluminum coating. The monopole aluminum nanoantenna of 50 nm width and 20 nm curvature radius has been fabricated by focused ion beam milling. The antenna is excited by the near field of the fiber probe. The antennas have been modeled using CST Microwave Studio. Figure 15 shows the antenna resonances for a wavelength $\lambda = 514$ nm and variable antenna length. The simulations have been validated by single molecule fluorescence measurements.

By coupling a poly[2-methoxy-5-(2'-ethyl-hexyloxy)-p-phenylene vinylene] (MEH-PPV) polymer to resonance-tuned silver nanoantenna arrays, the enhanced photoluminescence of the MEH-PPV/silver nanoantennae due to an energy transfer effect in the surface plasmon resonance coupling between the MEH-PPV and silver efficient solar cells for photon harvesting can be realized [47].

Bowtie nanoantennas consisting of gold triangles with triangle lengths of 75 nm and gaps ranging from 16 nm to 488 nm have been fabricated and investigated in [48]. Figure 16 shows two samples of bowtie antennas with gaps of 20 nm and 285 nm. The Au films are 20 nm thick with a 5 nm Cr adhesion layer and were deposited onto an indium tin oxide coated fused silica coverslip. Optical excitation of the bowtie structures excites the plasmon resonance of the structure, which could be sensed in the wavelength dependence of the scattering spectra.

Superconducting Antennas

Using superconductors allows the realization of superdirectivity antennas, addressed in the "Physical Constraints in Antenna Integration" section, of extremely small size. Furthermore, there are numerous

interesting applications of superconductors for antennas. Superconductors show superior properties, such as low power loss, low attenuation, and low noise level [49]. Superconductors allow us to realize extremely small antennas that exhibit a high radiation quality factor [50]. Superconducting antennas are well suited for the combination with Josephson-effect-based radiation detectors [51]. Superconducting quantum interference devices (SQUIDs) are extremely sensitive magnetic field sensors and active magnetic antennas applicable from dc to several 100 MHz [52], [53]. An electrically small active antenna for the frequency range 50–500 MHz, consisting of a $YBa_2Cu_3O_7$ half-loop plane antenna and a 200 element SQUID array amplifier is described in [54].

In [55] and [56], a mixer using a superconductor-insulator-superconductor (SIS) quasiparticle structure is integrated with a double-dipole antenna shown in Figure 17. The receiver operates at 500 GHz, 550–650 GHz, and 1.8 THz. This single-chip superconducting integrated receiver has been developed for the Terahertz Limb Sounder (TELIS) balloon project and is intended to measure a variety of stratosphere trace gases is presented.

By exciting a bow-tie antenna structure of a high temperature superconducting $YBa_2Cu_3O_{7-\delta}$ thin film dipole antenna on MgO substrate with 100 fs, 750 nm laser pulses, the radiation of terahertz pulses from the bow-tie antenna could be affected [57].

Hot-spot generation in the superconductor allows fast and ultrasensitive optical detection [58]. A photon incident on a superconducting nanowire or nanoribbon yields a temporary generation of a resistive barrier across the nanowire or the nanoribbon and results in a voltage pulse. The decay time is in the order of 30 ps. Superconducting nanowire single photon detectors exhibit broad wavelength response, short reset time, and low noise and, therefore, are promising candidates to replace other single photon detectors, like avalanche photodiodes in applications such as free-space optical communications, quantum cryptography networks, and quantum computation [59], [60]. Superconducting niobium nitride (NbN) nanowire single-photon detectors with silver optical antennas for free-space coupling were designed in [61]. Figure 18 shows the schematics of the device cross section exhibiting silver subwavelength grating between adjacent NbN nanowires. 100 nm wide NbN nanowires with 200 nm pitch on sapphire substrate are used. Light of 1,550 nm wavelength is incident from the bottom through the antireflection coating (ARC). Simulation results have shown a light absorption as high as 96% for TM polarization.

Carbon Nanotube Antennas

CNTs facilitate an extreme miniaturization due to slow wave propagation effects [62]. CNTs exhibit

Using superconductors allows the realization of superdirectivity antennas, and there are numerous interesting applications of superconductors for antennas.

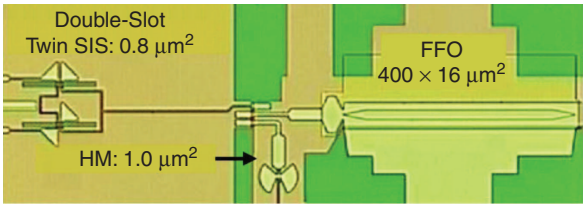

Figure 17. *Microphotograph of the central part of the superconducting integrated chip with double slot antenna [56].*

exceptional electron transport properties, yielding ballistic carrier transport at room temperature with a mean free path of around 0.7 μm and a carrier mobility of 10,000 cm^2/Vs [63], [64]. Due to the slow-wave propagation of electromagnetic waves in CNT structures, the wavelength of electromagnetic waves propagating in CNT structures is considerably smaller than the free-space wavelength. This effect occurs due to quantum transport effects in the CNT yielding a quantum capacitance and a kinetic inductance in addition to the geometric capacitance and inductance [65], [66]. In [65]–[67], a simplified equivalent circuit model of a CNT over ground according to Figure 19 is presented with a kinetic inductance per unit of length

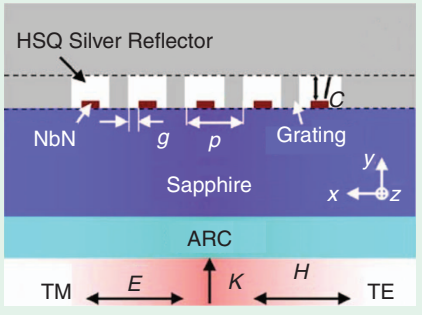

Figure 18. *Niobium nitride nanowire single-photon detectors integrated with silver optical antennas [61].*

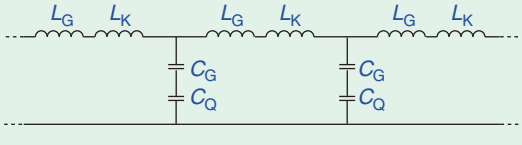

Figure 19. *Equivalent circuit model of a carbon nanotube over metallic ground plane.*

CNTs exhibit a very high inductance per unit length due to the high kinetic energy of the electrons.

L_K and a quantum capacitance per unit of length C_Q in addition to the geometry-based inductance and capacitance per unit of length L_G and C_G, respectively. CNTs exhibit a very high inductance per unit length due to the high kinetic energy of the electrons [68]. The high inductance results in an electromagnetic slow-wave propagation along a CNT transmission line configuration with a phase velocity in the order of $c_0/100$ to $c_0/50$ [69], where c_0 is the speed of light in free space. CNT nanoantennas much shorter than the operating wavelength can be brought into resonance and potentially be used as radiation elements [67]. A CNT nanoantenna is usually an electrically extremely short antenna, that is, it is considerably shorter than the free-space wavelength.

The appearance of slow waves makes CNT antennas interesting for wireless communication between circuits at the micro- and nanoscale or between nanocircuits and the macroscopic environment [67], [70]. Figure 20 shows a schematic drawing of a CNT dipole antenna.

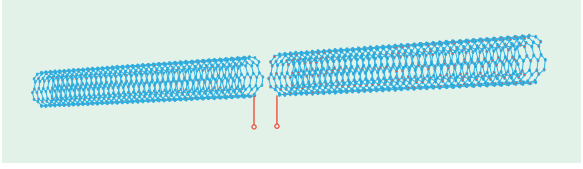

Figure 20. *Carbon nanotube dipole antenna.*

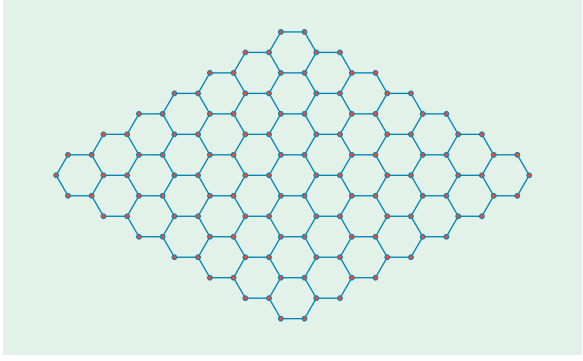

Figure 21. *Structure of a graphene layer.*

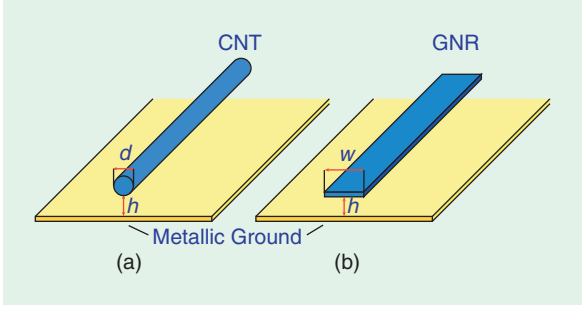

Figure 22. *Nanopatch antenna based (a) on a carbon nanotube and (b) on a graphene nanoribbon (GNR).*

In [71] an analytic expression for the surface conductance of a single-walled CNT was given that can be incorporated into the integral equations to account for the specific electron transport properties. In [72] and [73], copper and carbon dipole nanoantennas are investigated using modified Hallén and Pocklington integral equations, which incorporate the CNT surface conductance. It was found that CNT dipoles start to go into resonance at much lower frequencies than initially assumed. This can be explained from the fact that electromagnetic waves are propagating along CNTs, forming surface plasmons, which have a reduced propagation velocity and, thus, have shorter wavelengths. So, CNT dipoles with several micrometers in length start to resonate in the low terahertz region, where the wavelengths are 50–100 times longer compared to the length of the CNT dipole. The fundamental properties of nanotube antennas and the question for wireless data transfer at the nanoscale have been discussed in [74]. Wang et.al. investigated random arrays of aligned CNTs [75].

Linear nanoscale dipole antennas, either made of metal such as gold or silver or CNTs, have been investigated [68], [76]. Due to the extremely high aspect ratio (length/cross sectional area), both metal nanowires as well as CNTs have ac resistances per unit length in the order of several kiloohm per micrometer [76]. This high resistance causes high-conduction losses and thus seriously decreases the efficiency and the achievable gain of nanoantennas. In [68], the efficiency of a CNT dipole antenna is estimated to be in the range of –60 to –90 dB, which results from the high-conductance losses. The situation in the case of metal nanoantennas is similar. Although low-power levels are sufficient in modern communication links, the inherent loss introduced by metallic or CNT nanoantennas limits their applicability considerably. One approach to bypass the resistance problem could be the usage of arrays of nanoantennas or a bundle of parallel nanowires. In this case, the resistance can be decreased to an acceptable value; however, the slow-wave effect is lost, as discussed in [77]. Therefore, by an appropriate choice of geometry and the number of nanowires, the properties of nanoantenna structures have to be optimized.

Graphene Antennas

A promising alternative to CNT antennas could be planar structures such as two-dimensional (2-D) graphene layers. Graphene is a 2-D material consisting of a monoatomic layer of carbon atoms ordered in a honeycomb structure, as depicted in Figure 21 [78]–[80]. It exhibits an excellent crystal quality and unique

electronic properties [81]. Morozov et.al. have shown that electron-phonon scattering in graphene is so weak that room temperature electron mobilities as high as 200,000 cm^2/Vs can be expected if extrinsic disorder is eliminated [82].

Like CNTs, graphene also exhibits excellent conductivity and slow wave properties [83], [84]. The achievable slow-wave effect in plasmon modes is in the order of $c_0/100$. At terahertz frequencies, a population inversion in the graphene layer can be realized by optical pumping or forward bias, which yields an amplification of the surface plasmon. Graphene allows the realization of planar structures and active circuits [85].

Figure 22 shows patch antennas based on CNTs and graphene nanoribbons (GNRs). Theoretical investigations have shown that antennas with sizes in the order of several hundred nanometers are suitable to radiate electromagnetic waves in the terahertz band, that is, 0.1–1 THz [86].

Graphene has also been used as substrate for metallic antennas. In [87], metallic dipole antennas and arrays of dipole antennas have been paterned on a graphene layer. The antennas have been operated at 120 GHz. Using the high-resistivity and low-resistivity state of the graphene, the antenna radiation patterns could be controlled.

Alternative Materials and Fabrication Techniques

The antennas described previously are generally fabricated with conventional technologies, namely evaporation of the metallic films followed by patterning via photo- or electron-lithography. In the CNT or graphene case, the conductive layers have to be grown epitaxially on the given substrate. Especially when small dimensions are required, as for the nanometer gaps required in the plasmonic structures shown in the "Antennas in Plasmonic Devices" section or in the nanometer scale MOM diodes of the "Integration of Antennas with MOM Diodes section, a very interesting alternative could be offered by nanotransfer techniques [88]–[91].

The principle is illustrated in Figure 23. A mold is first fabricated holding a given pattern, which can contain nanometer features. One can use silicon, quartz, nickel, or even a flexible polymer like PDMS as mold material. Structures of few nanometer dimensions can also be realized using heterostructures from compound semiconductors like GaAs and AlGaAs [39], [40], [92]. The mold is then coated with a material that is comparable to an ink, which is transferred to the substrate by bringing the mold in contact with the substrate. Commonly, the mold is coated with an antisticking layer and/or the substrate is modified with a self-assembled monolayer (SAM) acting as covalent glue promoting the adhesion of the ink. Only the elevated surfaces of the mold come into contact with the substrate. Thus, during separation, the material present on such surfaces sticks to the substrate and is selectively transferred from mold to substrate.

A promising alternative to CNT antennas could be planar structures such as two-dimensional graphene layers.

Figure 24 presents the transferred metal pads, exhibiting a gap featuring line separations down to approximately 9 nm. The structures could be transferred along the complete length of the mold (approximately 4 m) with an efficiency of about 80%. Structures containing several lines separated by nanometer gaps have also been realized [50]. While most of the work so far has concentrated on the transfer of metallic films, preliminary indications suggest the possibility of transferring a complete stack, for instance a MOM diode. The advantage of the nanotransfer technique is that a single mold can be used several times, thus providing a cost-effective nanometer-scale fabrication

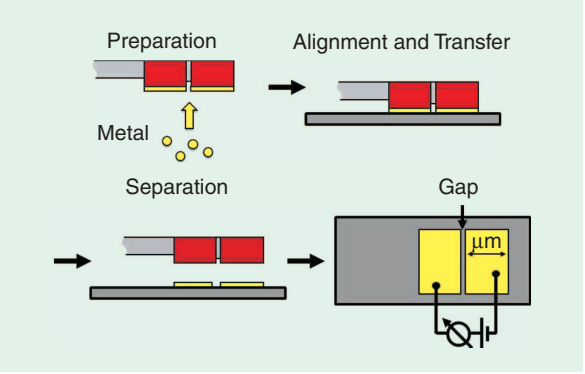

Figure 23. *Schematic of direct metal-transfer. A metal-coated high-esolution heterostructure is pressed onto a substrate, thereby creating nanometer-separated electrodes.*

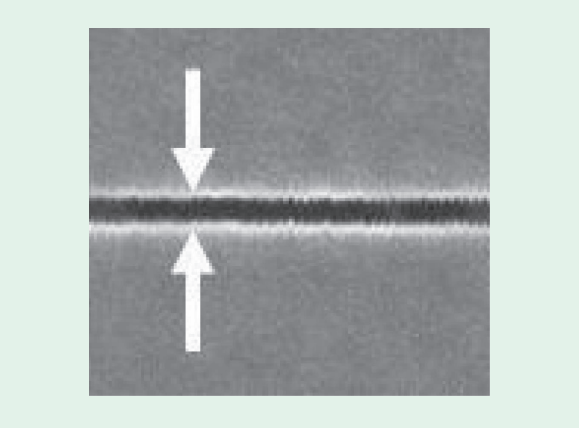

Figure 24. *Transfer metal pads with a gap of a few nanometers.*

TABLE 1. Comparison between tags based on conductive ink and on aluminum.

	Paramod VLT Worst-case	Paramod VLT Best-case	Aluminium
Layer thickness [μm]	25.4 (1.0 mils)	25.4 (1.0 mils)	85.00
Bulk conductivity[1,2] [S/m]	26.25e6	78.74e6	38e6
Coil resistance R (dc) [Ω]	3.94	2.57	2.98
Inductance L [μH]	4.47	4.39	4.37
Parasitic capacitance C_p [pF]	4.09	4.51	4.37
Resonance cap. C_g [pF]	26.74	26.87	27.13
Min. field strength H_{min} [A/m]	0.0285	0.0233	0.0248
Powering range x_{max} [m]	1.00	1.07	1.05
Q-factor	50.336	61.645	57.764

[1]Texas Instruments, *Tag-it TI-RFID Transponder Specifications*, www.ti.com
[2]Paralec, *Paramod VLT Inks Specifications*, www.paralec.com

capability. In addition, it is possible to repeat the transfer processes at different locations of the substrate, opening the way for large area applications. An alternative route to the fabrication of antenna structures for monolithic integration is provided through printing, or, in general, solution-based, techniques. In this case, the conductive material is mixed with a solvent and deposited on the substrate via ink jet printing, spray coating, or from various forms of coating (such as doctor blade or roll-to-roll). The most common example is provided by conductive inks used in the fabrication of RFID antennas. To verify that conductive polymeric material can be used for RFID tags working at 13.56 MHz, a comparison between standard aluminum antennas and antennas based on conductive inks has been performed via electromagnetic simulations [93]. The antenna coil is modeled by the inductance L of the coil in series with a resistor R (representing the ohmic losses in the coil that are not negligible when using materials with low conductivity) and a voltage source; these three components are connected in parallel with a capacitor. As reference antenna for the comparison, a commercial tag produced by Texas Instruments has been considered. The specifications of the conductive ink have been taken from a commercial product of Paralec called Paramod VLT[2], which is a blend of polymers and silver flakes. In Table 1, the results extracted from the simulations of the tags based on conductive ink are compared to the one based on aluminum. As can be seen, the performance of the antennas based on conductive ink matches that of the more standard one, as also confirmed by experiments. The minimum field strength H_{min} represents the magnetic field strength required for providing a voltage of 2.5 V to the tag chip, which is represented by a load resistance of 40 kΩ The powering range x_{max} is the maximal distance between the reader and the tag for which the minimum field strength H_{min} can be provided by the reader to the tag. For this calculation, a reference reader is assumed with a circular coil of radius 25 cm and a current-winding product of 1 A. In our study, we could also show that antennas may be printed using a conductive polymer, although the powering range is then reduced to a few centimeters due to the poor conductivity of the polymer compared to conductive inks and metals. The advantage of solution-based processes is that they provide the capability for large area fabrication on unconventional substrates, such as glass, plastic, textile, or even paper. Among the various available techniques, spray coating is very appealing because of its versatility, simplicity, and reduced cost [94], [95]. In addition, spray coated films can be conformed very nicely to nonuniform surfaces, such as in the realization of CMOS imagers with sprayed organic photodetectors. A very interesting and promising technology involves the CNTs described previously. By mixing a multitude of such nanotubes with a solvent, it is possible to prepare a solution that can be deposited with the above-mentioned techniques. Depending on the electrical characteristic of the embedded nanotube, one can obtain a semiconducting or a metallic film. Such films can be used, respectively, as active layers of thin film transistors or as electrodes/antennas [96]–[98]. A view of a CNT network is provided in Figure 25. A very attractive possibility offered by solution-based processes is to combine passive and active components as needed, for instance, in RFIDs.

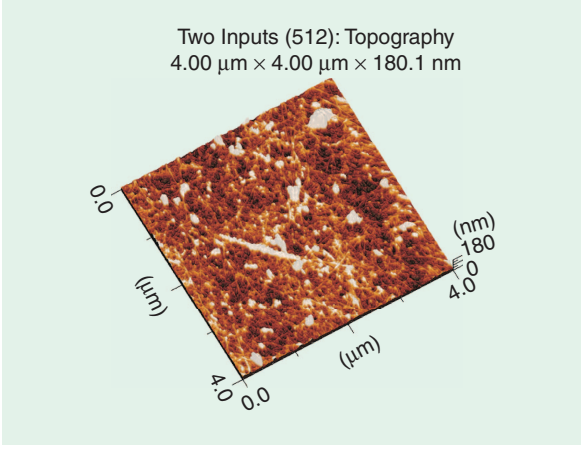

Figure 25. *Automatic force microscope picture of a network of single wall carbon nanotubes. The larger dots are clusters of nonseparated nanotubes.*

As shown recently by the micro- and nanoelectronics research center Interuniversity Microelectronics Centre (IMEC), a full organic RFID operating at 13.5 MHz can be fabricated on plastic using roll-to-roll technologies. The electronic components (rectifier, transistors, and memories) are based on conductive polymers, while the antenna was realized using conductive inks. Using CNT networks, one could probably improve the RFID performance and realize the complete RFID out of just one material system.

Conclusion and Outlook

As the structure size of circuit devices and components is continuously decreasing, the same will hold for antennas and radiation elements used in ICs for on-chip and chip-to-chip communication. Following the general scaling trend, on-chip antennas will soon enter the micrometer and even the nanometer regime.

Integrated antennas based on nanoelectronics provide a tremendous potential for the realization of novel devices and systems from dc up to the optical range. The applications will cover wireless intrachip and interchip transmission at Gb/s rates, field sensors, and photon harvesting systems.

Intrachip and interchip wireless broadband communication at mm-wave carrier frequencies can be realized in CMOS technology and will allow the transfer of Gb/s data rates. Using segmented ground metallizations as antenna elements allows the integration of antenna structures without additional chip-area consumption. A further size reduction of antenna structures will be possible by integration of CNT and graphene antenna structures. This will be interesting in connection with future RF CNT and graphene field effect transistors (FETs) and graphene-based ICs. With the advancement of miniaturization, MIMO systems using space multiplexing may also be realized.

Plasmonic antennas will facilitate high-speed optical communications and light energy harvesting. Superconducting devices allow the realization of sensitive and fast detectors from dc to optical frequencies. Alternative materials and fabrication techniques will open up further possibilities.

Acknowledgments

This article is based on research projects funded by the Deutsche Forschungsgemeinschaft, the TUM Institute of Advanced Study, and the U.S. Office of Naval Research.

References

[1] L. Pierantoni, "RF nanotechnology—Concept, birth, mission, and perspectives," *IEEE Microwave Mag.*, vol. 11, no. 4, pp. 130–137, June 2010.

[2] P. Russer and N. Fichtner, "Nanoelectronics in radio-frequency technology," *IEEE Microwave Mag.*, vol. 11, no. 3, pp. 119–135, May 2010.

[3] J. M. Jornet and I. F. Akyildiz, "Channel capacity of electromagnetic nanonetworks in the terahertz band," in *Proc. IEEE Int. Conf. Communications (ICC'10)*, May 2010.

[4] E. Kasper, D. Kissinger, P. Russer, and R. Weigel, "High speeds in a single chip," *IEEE Microwave*, vol. 10, no. 7, pp. 28–33, Dec. 2009.

[5] A. Niknejad, "Siliconization of 60 GHz," *IEEE Microwave*, vol. 11, no. 1, pp. 78–85, Feb. 2010.

[6] P. Russer, "Si and SiGe millimeter-wave integrated circuits," *IEEE Trans. Microwave Theory Tech.*, vol. 46, no. 5, pp. 590–603, May 1998.

[7] L. J. Chu, "Physical limitations of omnidirectional antennas," Res. Lab. Electron., Massachusetts Inst. Technol., Tech. Rep. 64, 1948.

[8] H. A. Wheeler, "Fundamental limitations of small antennas," *Proc. IRE*, vol. 35, pp. 1479–1484, Dec. 1947.

[9] H. Wheeler, "Small antennas," *IEEE Trans. Antennas Propagat.*, vol. 23, no. 4, pp. 462–469, July 1975.

[10] S. Best, "A discussion on the properties of electrically small self-resonant wire antennas," *IEEE Antennas Propagat. Mag.*, vol. 46, no. 6, pp. 9–22, Dec. 2004.

[11] S. Best, "A discussion on power factor, quality factor and efficiency of small antennas," in *Proc. IEEE Antennas and Propagation Society Int. Symp.*, June 2007, pp. 2269–2272.

[12] M. Gustafsson, C. Sohl, and G. Kristensson, "Physical limitations on antennas of arbitrary shape," *Proc. R. Soc. A: Math. Phys. Eng. Sci.*, vol. 463, no. 2086, pp. 2589–2607, Oct. 2007.

[13] M. Gustafsson, C. Sohl, and G. Kristensson, "Illustrations of new physical bounds on linearly polarized antennas," *IEEE Trans. Antennas Propagat.*, vol. 57, no. 5, pp. 1319–1327, May 2009.

[14] S. A. Schelkunoff, "A mathematical theory of linear arrays," *Bell Syst. Tech. J.*, vol. 22, no. 1, pp. 80–107, Jan. 1943.

[15] N. Yaru, "A note on super-gain antenna arrays," *Proc. IRE*, vol. 39, no. 9, pp. 1081–1085, Sept. 1951.

[16] A. Goldsmith, S. Jafar, N. Jindal, and S. Vishwanath, "Capacity limits of MIMO channels," *IEEE J. Select. Areas Commun.*, vol. 21, no. 5, pp. 684–702, June 2003.

[17] M. Migliore, "An intuitive electromagnetic approach to MIMO communication systems," *IEEE Antennas Propagat. Mag.*, vol. 48, no. 3, pp. 128–137, June 2006.

[18] J. Wallace and M. Jensen, "Mutual coupling in MIMO wireless systems: A rigorous network theory analysis," *IEEE Trans. Wireless Commun.*, vol. 3, no. 4, pp. 1317–1325, July 2004.

[19] F. Gruber and E. Marengo, "New aspects of electromagnetic information theory for wireless and antenna systems," *IEEE Trans. Antennas Propagat.*, vol. 56, no. 11, pp. 3470–3484, Nov. 2008.

[20] M. T. Ivrlac and J. A. Nossek, "Toward a circuit theory of communication," *IEEE Trans. Circuits Syst. I*, vol. 57, no. 7, pp. 1663–1683, July 2010.

[21] A. Rosen, M. Caulton, P. Stabile, A. M. Gombar, W. M. Janton, C. P. Wu, J. F. Corboy, and C. W. Magee, "Silicon as a millimeter-wave monolithically integrated substrate," *RCA Rev.*, vol. 42, pp. 633–660, Dec. 1981.

[22] J. F. Luy and P. Russer, *Silicon-Based Millimeter-Wave Devices (Springer Series in Electronics and Photonics, vol. 32)*. Berlin, Heidelberg, New York: Springer-Verlag, 1994.

[23] P. Russer and E. Biebl, "Fundamentals," in *Silicon-Based Millimeter-Wave Devices (Springer Series in Electronics and Photonics)*, J. F. Luy and P. Russer, Eds. Berlin, Heidelberg, New York: Springer-Verlag, 1994, no. 32, pp. 149–192.

[24] B. Floyd, C. Hung, and K. Kenneth, "A 15-GHz wireless interconnect implemented in a 0.18-µm CMOS technology using integrated transmitters, receivers, and antennas," in *IEEE Symp. VLSI Circuits, Dig. Technical Papers*, July 2001, pp. 155–158.

[25] K. O, K. Kim, B. Floyd, et al., "The feasibility of on-chip interconnection using antennas," in *Proc. IEEE/ACM Int. Conf. Computer-Aided Design (ICCAD'05)*, Nov. 2005, pp. 979–984.

[26] J. Branch, X. Guo, L. Gao, A. Sugavanam, J. Lin, and K. O, "Wireless communication in a flip-chip package using integrated antennas on silicon substrates," *IEEE Electron Device Lett.*, vol. 26, no. 2, pp. 115–117, Feb. 2005.

[27] K. O, K. Kim, B. Floyd, et al., "On-chip antennas in silicon ICs and their application," *IEEE Trans. Electron Devices*, vol. 52, no. 7, pp. 1312–1323, July 2005.

[28] K. O, K. Kim, B. Floyd, et al., "Silicon integrated circuits incorporating antennas," in *Proc. IEEE Custom Integrated Circuits Conf. (CICC'06)*, Sept. 2006, pp. 473–480.

[29] M. Sun, Y. P. Zhang, G. X. Zheng, and W. Yin, "Performance of intra-chip wireless interconnect using on-chip antennas and UWB radios," *IEEE Trans. Antennas Propagat.*, vol. 57, no. 9, pp. 2756–2762, Sept. 2009.

[30] Y. P. Zhang, Z. M. Chen, and M. Sun, "Propagation mechanisms of radio waves over intra-chip channels with integrated antennas: Frequency-domain measurements and time-domain analysis," *IEEE Trans. Antennas Propagat.*, vol. 55, no. 10, pp. 2900–2906, Oct. 2007.

[31] Z. M. Chen and Y. Zhang, "Inter-chip wireless communication channel: Measurement, characterization, and modeling," *IEEE Trans. Antennas Propagat.*, vol. 55, no. 3, pp. 978–986, Mar. 2007.

[32] H. Yordanov and P. Russer, "Integrated on-chip antennas using CMOS ground planes," in *Proc. 10th Topical Meeting on Silicon Monolithic Integrated Circuits in RF Systems*, New Orleans, LA, Jan. 2010, pp. 53–56.

[33] H. Yordanov and P. Russer, "Area-efficient integrated antennas for inter-chip communication," in *Proc. 40th European Microwave Conf. (EuMC'10)*, Paris, France, Sept. 2010.

[34] C. Fumeaux, G. D. Boreman, W. Herrmann, H. Rothuizen, and F. K. Kneubühl, "Polarization response of asymmetric-spiral infrared antennas," *Appl. Opt.*, vol. 36, no. 25, pp. 6485–6490, Sept. 1997.

[35] P. Esfandiari, G. Bernstein, P. Fay, W. Porod, et al., "Tunable antenna-coupled metal-oxide-metal (MOM) uncooled IR detector," *Proc. SPIE*, vol. 5783, pp. 471–482, May 2005.

[36] J. A. Bean, B. Tiwari, G. H. Bernstein, P. Fay, and W. Porod, "Thermal infrared detection using dipole antenna-coupled metal-oxide-metal diodes," *J. Vacuum Sci. Technol. B: Microelectron. Nanometer Struct.*, vol. 27, p. 11, Jan. 2009.

[37] B. Tiwari, J. A. Bean, G. Szakmány, G. H. Bernstein, P. Fay, and W. Porod, "Controlled etching and regrowth of tunnel oxide for antenna-coupled metal-oxide-metal diodes," *J. Vacuum Sci. Technol. B: Microelectron. Nanometer Struct.*, vol. 27, pp. 2153–2160, Sept. 2009.

[38] J. A. Bean, B. Tiwari, G. Szakmány, G. H. Bernstein, P. Fay, and W. Porod, "Antenna length and polarization response of antenna-coupled MOM diode infrared detectors," *Infrared Phys. Technol.*, vol. 53, no. 3, pp. 182–185, May 2010.

[39] S. Harrer, S. Strobel, G. Scarpa, G. Abstreiter, M. Tornow, and P. Lugli, "Room temperature nanoimprint lithography using molds fabricated by molecular beam epitaxy," *IEEE Trans. Nanotechnol.*, vol. 7, no. 3, pp. 363–370, May 2008.

[40] S. Harrer, S. Strobel, G. Penso Blanco, G. Scarpa, G. Abstreiter, M. Tornow, and P. Lugli, "Technology assessment of a novel high-yield lithographic technique for sub-15-nm direct nanotransfer printing of nanogap electrodes," *IEEE Trans. Nanotechnol.*, vol. 8, no. 6, pp. 662–670, Nov. 2009.

[41] W. Barnes, A. Dereux, and T. Ebbesen, "Surface plasmon subwavelength optics," *Nature*, vol. 424, pp. 824–830, Nov. 2003.

[42] R. Zia, J. A. Schuller, A. Chandran, and M. L. Brongersma, "Plasmonics: The next chip-scale technology," *Mater. Today*, vol. 9, no. 7–8, pp. 20–27, July 2006.

[43] S. Maier, *Plasmonics: Fundamentals and Applications*. New York: Springer-Verlag, 2007.

[44] M. L. Brongersma, "Plasmonics: Engineering optical nanoantennas," *Nat. Photon.*, vol. 2, no. 5, pp. 270–272, May 2008.

[45] J. Fujikata, J. Ushida, D. Okamoto, A. Gomyo, K. Nishi, T. Tsuchizawa, T. Watanabe, K. Yamada, S. Itabashi, and K. Ohashi, "Si nano-photodiode with a surface-plasmon antenna for SiON waveguide-integrated structure," in *Proc. 20th Annu. Meeting IEEE Lasers and Electro-Optics Society (LEOS'07)*, 2007, pp. 929–930.

[46] T. H. Taminiau, R. J. Moerland, F. B. Segerink, L. Kuipers, and N. F. V. Hulst, "λ/4 resonance of an optical monopole antenna probed by single molecule fluorescence," *Nano Lett.*, vol. 7, no. 1, pp. 28–33, Jan. 2007.

[47] L. Si, T. Qiu, W. Zhang, and P. K. Chu, "Plasmon-enhanced luminescence in MEH-PPV coupled silver nanoantenna arrays and the potential for photovoltaics," in *Proc. 2010 3rd Int. Nanoelectronics Conf. (INEC'10)*, Hong Kong, China, pp. 1345–1346.

[48] D. P. Fromm, A. Sundaramurthy, P. J. Schuck, G. Kino, and W. E. Moerner, "Gap-dependent optical coupling of single "bowtie" nanoantennas resonant in the visible," *Nano Lett.*, vol. 4, no. 5, pp. 957–961, May 2004.

[49] M. Amir, F. Chebbara, T. Fortaki, and L. Djouane, "Analysis of rectangular microstrip antenna using high temperature superconducting (HTS) patch," in *Proc. 2nd Int. Conf. Signals, Circuits and Systems (SCS'08)*, 2008, pp. 1–4.

[50] R. Hansen, *Electrically Small, Superdirective and Superconducting Antennas*. New York: Wiley, 2006.

[51] K. Kang, I. Song, Y. S. Ha, S. Han, G. Y. Sung, I. Song, and G. Park, "Microwave radiation and sensing of Josephson junction with the log-periodic toothed trapezoid antenna of high Tc superconducting films," *IEEE Trans. Appl. Superconduct.*, vol. 9, no. 2, pp. 3074–3076, June 1999.

[52] D. Drung, C. Assmann, J. Beyer, A. Kirste, M. Peters, F. Ruede, and T. Schurig, "Highly sensitive and easy-to-use SQUID sensors," *IEEE Trans. Appl. Superconduct.*, vol. 17, no. 2, pp. 699–704, June 2007.

[53] M. Matsuda, K. Nakamura, H. Mikami, and S. Kuriki, "Fabrication of magnetometers with multiple-SQUID arrays," *IEEE Trans. Appl. Superconduct.*, vol. 15, no. 2, pp. 817–820, June 2005.

[54] J. Luine, L. Abelson, D. Brundrett, J. Burch, E. Dantsker, K. Hummer, G. Kerber, M. Wire, K. Yokoyama, D. Bowling, M. Neel, S. Hubbell, and K. Li, "Application of a dc SQUID array amplifier to an electrically small active antenna," *IEEE Trans. Appl. Superconduct.*, vol. 9, no. 2, pp. 4141–4144, June 1999.

[55] V. Koshelets, S. Shitov, A. Ermakov, L. Filippenko, O. Koryukin, A. Khudchenko, M. Torgashin, P. Yagoubov, R. Hoogeveen, and O. Pylypenko, "Superconducting integrated receiver for TELIS," *IEEE Trans. Appl. Superconduct.*, vol. 15, no. 2, pp. 960–963, June 2005.

[56] V. Koshelets, A. Ermakov, L. Filippenko, A. Khudchenko, O. Kiselev, A. Sobolev, M. Torgashin, P. Yagoubov, R. Hoogeveen, and W. Wild, "Superconducting integrated submillimeter receiver for TELIS," *IEEE Trans. Appl. Superconduct.*, vol. 17, no. 2, pp. 336–342, June 2007.

[57] S. Pai and C. Chi, "Waveforms of terahertz radiation emitted from superconducting dipole antenna," in *Proc. 2007 IEEE/LEOS Int. Conf. Optical MEMS and Nanophotonics*, pp. 19–20.

[58] G. N. Gol'tsman, O. Okunev, G. Chulkova, A. Lipatov, A. Semenov, K. Smirnov, B. Voronov, A. Dzardanov, C. Williams, and R. Sobolewski, "Picosecond superconducting single-photon optical detector," *Appl. Phys. Lett.*, vol. 79, no. 6, p. 705, Aug. 2001.

[59] V. Anant, A. J. Kerman, E. A. Dauler, and J. KW, "Optical properties of superconducting nanowire single-photon detectors," *Nature*, vol. 409, pp. 46–52, June 2001.

[60] H. Takesue, S. W. Nam, Q. Zhang, R. H. Hadfield, T. Honjo, K. Tamaki, and Y. Yamamoto, "Quantum key distribution over a 40-dB channel loss using superconducting single-photon detectors," *Nat. Photon.*, vol. 1, no. 6, pp. 343–348, June 2007.

[61] X. Hu, C. Holzwarth, D. Masciarelli, E. Dauler, and K. Berggren, "Efficiently coupling light to superconducting nanowire single-photon detectors," *IEEE Trans. Appl. Superconduct.*, vol. 19, no. 3, pp. 336–340, June 2009.

[62] G. Hanson, "Fundamental transmitting properties of carbon nanotube antennas," *IEEE Trans. Antennas Propagat.*, vol. 53, no. 11, pp. 3426–3435, Nov. 2005.

[63] C. Dekker, "Carbon nanotubes as molecular quantum wires," *Phys. Today*, vol. 52, pp. 22–28, May 1999.

[64] M. Dragoman, G. Konstantinidis, A. Kostopoulos, D. Dragoman, D. Neculoiu, R. Buiculescu, R. Plana, F. Coccetti, and H. Hartnagel, "Multiple negative resistances in trenched structures bridged with carbon nanotubes," *Appl. Phys. Lett.*, vol. 93, no. 4, pp. 043117–043117-3, July 2008.

[65] P. Burke, "An RF circuit model for carbon nanotubes," in *Proc. 2002 2nd IEEE Conf. Nanotechnology (IEEE-NANO'02), 2002*, pp. 393–396.

[66] P. Burke, "An RF circuit model for carbon nanotubes," *IEEE Trans. Nanotechnol.*, vol. 2, no. 1, pp. 55–58, Mar. 2003.

[67] N. Fichtner and P. Russer, "On the possibility of nanowire antennas," in *Proc. 36th European Microwave Conf.*, 2006, pp. 870–873.

[68] P. Burke, S. Li, and Z. Yu, "Quantitative theory of nanowire and nanotube antenna performance," *IEEE Trans. Nanotechnol.*, vol. 1, pp. 1–16, Aug. 2004.

[69] P. Burke, "Lüttinger liquid theory as a model of the gigahertz electrical properties of carbon nanotubes," *IEEE Trans. Nanotechnol.*, vol. 1, no. 3, pp. 129–144, Sept. 2002.

[70] S. Li, Z. Yu, C. Rutherglen, and P. J. Burke, "Electrical properties of 0.4 cm long single-walled carbon nanotubes," Aug. 2004.

[71] G. Slepyan, S. Maksimenko, A. Lakhtakia, O. Yevtushenko, and A. Gusakov, "Electrodynamics of carbon nanotubes: Dynamic conductivity, impedance boundary conditions, and surface wave propagation," *Phys. Rev. B*, vol. 60, no. 24, pp. 17136–17149, Dec. 1999.

[72] G. Hanson, "Fundamental transmitting properties of carbon nanotube antennas," *IEEE Trans. Antennas Propagat.*, vol. 53, no. 11, pp. 3426–3435, Nov. 2005.

[73] J. Hao and G. Hanson, "Carbon nanotube dipoles: Infrared and optical antenna properties," in *Proc. ACES*, Miami, FL, Mar. 2006, pp. 353–358.

[74] P. Burke, "Carbon nanotube devices for GHz to THz applications," *Proc. SPIE*, vol. 5593, pp. 52–61, Dec. 2003.

[75] Y. Wang, K. Kempa, B. Kimball, J. Carlson, G. Benham, W. Li, T. Kempa, J. Rybczynski, A. Herczynski, and Z. Ren, "Receiving and transmitting light-like radio waves: Antenna effects in arrays of aligned carbon nanotubes," *Appl. Phys. Lett.*, vol. 85, no. 13, pp. 2607–2609, Sept. 2004.

[76] C. Rutherglen and P. Burke, "Nanoelectromagnetics: Circuit and electromagnetic properties of carbon nanotubes," *Small*, vol. 5, no. 8, pp. 884–906, Apr. 2009.

[77] A. Attiya, "Lower frequency limit of carbon nanotube antenna," *Prog. Electromagn. Res.*, vol. 94, pp. 419–433, July 2009.

[78] K. S. Novoselov, A. K. Geim, S. V. Morozov, D. Jiang, Y. Zhang, S. V. Dubonos, I. V. Grigorieva, and A. A. Firsov, "Electric field effect in atomically thin carbon films," *Science*, vol. 306, no. 5696, pp. 666–669, Oct. 2004.

[79] A. K. Geim and K. S. Novoselov, "The rise of graphene," *Nat. Mater.*, vol. 6, pp. 183–191, Mar. 2007.

[80] A. K. Geim, "Graphene: Status and prospects," *Science*, vol. 324, no. 5934, pp. 1530–1534, June 2009.

[81] K. S. Novoselov, A. K. Geim, S. V. Morozov, D. Jiang, M. I. Grigorieva, S. V. Dubonos, and A. A. Firsov, "Two-dimensional gas of massless dirac fermions in graphene," *Nature*, vol. 438, pp. 197–200, Nov. 2005.

[82] S. V. Morozov, K. S. Novoselov, M. I. Katsnelson, F. Schedin, D. C. Elias, J. A. Jaszczak, and A. K. Geim, "Giant intrinsic carrier mobilities in graphene and its bilayer," *Phys. Rev. Lett.*, vol. 100, no. 1, pp. 16602–16605, Jan. 2008.

[83] F. Rana, "Graphen terahertz plasmon oscillators," *IEEE Trans. Nanotechnol.*, vol. 1, pp. 0–8, Jan. 2008

[84] G. W. Hanson, "Dyadic green's functions and guided surface waves for a surface conductivity model of graphene," *J. Appl. Phys.*, vol. 103, no. 6, pp. 064302–064302-8, Mar. 2008.

[85] J. Moon, D. Curtis, M. Hu, D. Wong, P. Campbell, G. Jernigan, J. L. Tedesco, B. VanMil, R. L. Myers-Ward, C. Eddy, Jr., et al., "Development toward wafer-scale graphene RF electronics," in *Proc. Topical Meeting Silicon Monolithic Integrated Circuits in RF Systems*, New Orleans, LA, Jan. 11–13, 2010, pp. 1–3.

[86] J. M. Jornet and I. F. Akyildiz, "Graphene-based nano-antennas for electromagnetic nanocommunications in the terahertz band," in *Proc. 4th European Conf. Antennas and Propagation (EUCAP'10)*, 2010.

[87] M. Dragoman, A. A. Muller, D. Dragoman, F. Coccetti, and R. Plana, "Terahertz antenna based on graphene," *J. Appl. Phys.*, vol. 107, no. 10, p. 104313, 2010.

[88] Y. N. Xia and G. M. Whitesides, "Soft lithography," *Angew. Chem. Int. Ed.*, vol. 37, no. 5, pp. 551–575, 1998.

[89] Y. L. Loo, R. L. Willett, K. W. Baldwin, and J. A. Rogers, "Additive, nanoscale patterning of metal films with a stamp and a surface chemistry mediated transfer process: Applications in plastic electronics," *Appl. Phys. Lett.*, vol. 81, pp. 562–564, July 2002.

[90] C. Kim, M. Shtein, and S. R. Forrest, "Nanolithography based on patterned metal transfer and its application to organic electronic devices," *Appl. Phys. Lett.*, vol. 80, pp. 4051–4053, May 2002.

[91] K. Felmet, Y. L. Loo, and Y. M. Sun, "Patterning conductive copper by nanotransfer printing," *Appl. Phys. Lett.*, vol. 85, pp. 3316–3318, Oct. 2004.

[92] S. Strobel, S. Harrer, G. P. Blanco, G. Scarpa, G. Abstreiter, P. Lugli, and M. Tornow, "Planar nanogap electrodes by direct nanotransfer printing," *Small*, vol. 5, pp. 579–582, 2009.

[93] P. Lugli, S. Bovelli, A. Di Carlo, M. Berliocchi, A. Bolognesi, and M. Manenti, "RFID: Ideas for future developments," in *Fields, Networks, Computational Methods and Systems in Modern Electrodynamics*, vol. 97, P. Russer and M. Mongiardo, Eds. New York: Springer-Verlag, 2004, p. 255.

[94] S. F. Tedde, J. Kern, T. Sterzl, J. Fürst, P. Lugli, and O. Hayden, "Fully spray coated organic photodiodes," *Nano Lett.*, vol. 9, no. 3, pp. 980–983, Feb. 2009.

[95] A. Abdellah, B. Fabel, P. Lugli, and G. Scarpa, "Spray deposition of organic semiconducting thin-films: Towards the fabrication of arbitrary shaped organic electronic devices," *Organic Electron.*, vol. 11, no. 6, pp. 1031–1038, June 2010.

[96] T. A. Elwi, H. M. Al-Rizzo, D. G. Rucker, E. Dervishi, Z. Li, and A. S. Biris, "Multi-walled carbon nanotube-based RF antennas," *Nanotechnology*, vol. 21, no. 4, p. 045301, Jan. 2010.

[97] J. A. Rogers, T. Someya, and Y. Huang, "Materials and mechanics for stretchable electronics," *Science*, vol. 327, no. 5973, pp. 1603–1607, Mar. 2010.

[98] Q. Cao and J. A. Rogers, "Ultrathin films of single-walled carbon nanotubes for electronics and sensors: A review of fundamental and applied aspects," *Adv. Mater.*, vol. 21, no. 1, pp. 29–53, 2008.